

# Oxygen measurements in stagnant lead–bismuth eutectic using electrochemical sensors

J. Konys, H. Muscher<sup>\*</sup>, Z. Voß, O. Wedemeyer

*Forschungszentrum Karlsruhe GmbH, Institute for Materials Research III, 76021 Karlsruhe, Germany*

## Abstract

Sensors are the major part of an active oxygen control system (OCS) to be used in ADS reactors employing lead bismuth eutectic (LBE). We tested Pt/air and Bi/Bi<sub>2</sub>O<sub>3</sub> probes based on yttria-stabilized zirconia (YSZ) solid electrolytes. The sensors were calibrated by evaluating the electromotive force (EMF) – temperature dependencies in oxygen un-/saturated stagnant LBE compared to the van't-Hoff's isotherm. Also, probe kinetics while changing the H<sub>2</sub>/H<sub>2</sub>O ratio was studied. Typical, reproducible curves are presented confirming attainment of oxygen equilibrium between the fluids. The sensor outputs are deterministic, predictable. Exceptional small drifts were due to interfacial kinetics, not to the sensors behavior. Simultaneous testing of several probes in one melt was performed. The sensors seemed to be qualified for large scale use.

© 2004 Elsevier B.V. All rights reserved.

## 1. Introduction

LBE can be corrosive to ADS structure materials (steels). OCS can lower corrosion by the formation of oxide scales, but at the same time liquid metal (LM) oxidation must be avoided [1]. Oxygen probes must be evaluated carefully for the loop operational conditions. This is done on a lab-scale. Such tests were performed with Bi/Bi<sub>2</sub>O<sub>3</sub> and Pt/air sensors using the modified EMF method presented first by Wagner [2]. Detailed descriptions are given in reviews [3,4]. Calculations regarding the EMF(*T*, *c*<sub>O</sub>) dependencies of particular sensor types are necessary for the calibration. Activity scaling for dissolved oxygen in LBE according to Borgstedt, Shmatko [4,5] was used here. Other approaches (i.e. listed in [6–8])

can also be adopted. Thermodynamic oxide data and oxygen solubilities must be considered for determining of *a*<sub>O</sub> in LBE [9–11]. For solutions obeying Henry's law *a*<sub>O</sub> in the melt can be equilibrated (fixed) via the gas phase *p*<sub>O<sub>2</sub></sub>. The H<sub>2</sub>/H<sub>2</sub>O-ratio determining *p*<sub>O<sub>2</sub></sub> was first introduced by Chipman [12] and extended treated in [13].

## 2. Theory

The scheme of our Bi/Bi<sub>2</sub>O<sub>3</sub> probe in LBE – with PbO as the oxide to be formed first in an oxygen saturated solution – is given as: (–) SS, Pb, PbO [YSZ], Bi, Bi<sub>2</sub>O<sub>3</sub>, Mo (+), where the oxidation and reduction processes are  $3\text{Pb} \rightarrow 3\text{Pb}^{2+} + 6\text{e}$ ,  $2\text{Bi}^{3+} + 6\text{e} \rightarrow 2\text{Bi}$ , respectively.

Note, oxygen O<sup>2–</sup> ions have no effect on the EMF for oxygen saturated LBE, the transfer of electrons from

<sup>\*</sup> Corresponding author. Fax: +49 7247 82 3956.

E-mail address: [heinrich.muscher@imf.fzk.de](mailto:heinrich.muscher@imf.fzk.de) (H. Muscher).

metallic lead towards Bi(III) cations is the infinitesimal redox process here. The global cell reaction is:  $2/3\text{Bi}_2\text{O}_3 + 2\text{Pb} \rightarrow 4/3\text{Bi} + 2\text{PbO}$ , with

$$\Delta G_{\text{ref}}^0 = RT \ln p_{\text{O}_2}^{\text{ref}} = \frac{2}{3} \Delta_f G_{\text{Bi}_2\text{O}_3}^0 \quad (\text{J/mol O}_2) \quad (1)$$

and

$$\begin{aligned} \Delta G_{\text{sample}}^0 &= RT \ln p_{\text{O}_2}^{\text{sample}} \\ &= 2\Delta_f G_{\text{PbO}}^0 - 2RT \ln a_{\text{Pb}} \\ &\quad + 2RT \ln \frac{C_{\text{O}}}{C_{\text{O}}^{\text{sat}}} \quad (\text{J/mol O}_2). \end{aligned} \quad (2)$$

Oxygen dissolved in LBE is supposed to be mono-atomic. Precipitation of PbO(s) begins at the saturation point (LBE's clogging). The  $a_{\text{Pb}}(T, p)$  effects for LBE were neglected, since published data for 550 and 575 °C exhibit an equality here within the limit of 0.01 and the  $x_{\text{Pb}}$  value remain constant in an eutectic alloy. Moreover, Agarwala's 550 °C/575 °C- $a_{\text{Pb}}(x_{\text{Pb}})$ -isotherms exhibit even equal activities in the neighborhood of the eutectic point,  $x_{\text{Pb}}$  being in between (0.3–0.6). The same is true for the constance of the partial and integral molar excess Gibbs free energies of the PbBi binary alloy components at this dedicated  $x_{\text{Pb}}$  region [14]. So, nearly no dependence on pressure can be expected, too. Using explicit data for Gibbs free energies of oxide formation, ranging from the standard 298 K to the melting point of PbO, (yellow, massicot,  $T_m = 1159$  K) or respectively to the transition point of two solid-crystalline  $\alpha$ - and  $\beta$ -Bi<sub>2</sub>O<sub>3</sub> (upper limit 1003 K, below the  $T_m$ ):

$$\begin{aligned} \Delta G_{\text{Bi}_2\text{O}_3}^0 &= -386790 + 188.95T, \\ \Delta G_{\text{PbO}}^0 &= -436850 + 197.99T \quad (\text{J/mol O}_2), \end{aligned} \quad (3)$$

the cell's EMF( $T$ ) can be estimated. Generally (an unsaturated solution, binary LBE) one obtains:

$$\begin{aligned} E &= \frac{1}{4F} \\ &\cdot \left( \frac{2}{3} \Delta_f G_{\text{Bi}_2\text{O}_3}^0 - 2\Delta_f G_{\text{PbO}}^0 + 2RT \ln a_{\text{Pb}} - 2RT \ln \frac{C_{\text{O}}}{C_{\text{O}}^{\text{sat}}} \right). \end{aligned} \quad (4)$$

Applying the Orlov's  $\ln C_{\text{O}}^{\text{sat}}(T)$  solubility dependence [1] the EMF( $T$ ) is given as

$$\begin{aligned} E(V) &= -0.2075 + 4.62 \times 10^{-4}T - 4.308 \times 10^{-5}T \\ &\quad \times \ln c_{\text{O,PbBi}} \text{ [wppm]}. \end{aligned} \quad (5)$$

It is important to point out that only the terminal Gibbs energy of solubility equal to the Gibbs energy the first oxide formation. In the case of unsaturated solutions in LBE  $\Delta G_{\text{sol}}^0$  according to:  $1/2\text{O}_{2(\text{g})} \rightleftharpoons [\text{O}]_{\text{PbBi}(l)}$  must be considered as:  $\Delta G_{\text{sol}}^0 = -RT \ln a_{[\text{O}]} / p_{\text{O}_2}^{1/2} = RT \ln p_{\text{O}_2}^{1/2} - RTx/x^{\text{sat}}$ .

How large the differences against the terminal (saturation) values are – this is not known; the need of relia-

ble, accurate data for  $\Delta G_{\text{sol}}^0$  in LBE is obvious [1]. A conversion of  $p_{\text{O}_2}$  into  $a_{\text{O}}$  of atomic oxygen dissolved in LBE could be simply done then. However, these missing data are only hypothetical and so they will not be pointed out here.

In contrast to the Bi/Bi<sub>2</sub>O<sub>3</sub> system, if the Pt/air direct electrode is adopted in LBE, lead is oxidised and oxygen reduced; the product – an equimolar sum of Pb<sup>2+</sup> and O<sup>2-</sup> ions – equals to the PbO, so the cell scheme becomes simply (–) SS, Pb, PbO |YSZ| Pt, air  $p_{\text{O}_2} = 0.21$  (+).

Using steam data of Barin ( $T > 298$  K), summarised as  $\Delta G_{\text{H}_2\text{O}}^0 = -487072 + 100.00T$  (J/mol O<sub>2</sub>), we got at first the useful dependencies of the EMFs on the temperature and the H<sub>2</sub>/H<sub>2</sub>O ratio:

$$\begin{aligned} \text{EMF}(T, p_{\text{H}_2}/p_{\text{H}_2\text{O}}, \text{ mV}) &= 1260.92 - 0.293T + 0.043T \\ &\quad \times \ln(p_{\text{H}_2}/p_{\text{H}_2\text{O}}) \quad \text{for Pt/air}, \end{aligned} \quad (6)$$

$$\begin{aligned} \text{EMF}(T, p_{\text{H}_2}/p_{\text{H}_2\text{O}}, \text{ mV}) &= 260 + 0.231T + 0.043T \\ &\quad \times \ln(p_{\text{H}_2}/p_{\text{H}_2\text{O}}) \quad \text{for Bi/Bi}_2\text{O}_3. \end{aligned} \quad (7)$$

With the help of Eq. (7) (identical derivation is applicable for In/In<sub>2</sub>O<sub>3</sub>, Sn/SnO<sub>2</sub> etc. [15]) asymptotic EMF( $\tau$ ) isotherm envelopes for describing our gas exchange tests were drawn. This allows to control oxygen in the LBE online the at a wide range of  $p_{\text{O}_2}$  beginning with the saturation.

### 3. Experimental

The design and setup of our sensors was presented in [16]. The KOSIMA-AT facility (Karlsruhe Oxygen Sensors in Molten Alloys Advanced Technology) has been setup for sensors evaluation tests. It allows to calibrate simultaneously probes immersed in the same stagnant melt parallel to the gas phase  $p_{\text{O}_2}$  measurements. The data acquisition/monitoring is computerised. For oxidation dry air was used while Ar/5%-H<sub>2</sub>-mix was the choice for reduction. To the latter, water was added using a thermostat at 7.4 °C. Keeping a constant total gas flow rate and changing only the flows of Ar and Ar/5%-H<sub>2</sub> the required H<sub>2</sub>/H<sub>2</sub>O ratios can be stepwise fixed. The gas mix is guided over a moisture sensor and then bubbled through the melt. After each measuring campaign, the LBE was deoxidised imposing a pre-selected Ar/H<sub>2</sub> dry gas bubbled through the melt for hours. The  $p_{\text{O}_2}$  of the outlet was detected by an industrial lambda- and another commercial ZIROX<sup>TM</sup> Pt/air-sensor (pre-heated to 750 °C). These  $p_{\text{O}_2}$  values were online correlated with the  $a_{\text{O}}$  in the LBE. The oxygen saturated solutions were prepared by dispersed bubbling

of dry air through the LBE. Details about gas exchange experiments are available in [6,9,17]. We reduced some possible sources of errors ( $H_2$ -diffusion) by the experimental design: tests were performed for medium  $H_2/H_2O$  ratios and the presence of argon raised the molecular weight of the mix. After several heating cycles gastightness was still given. Although temperature was kept constant along the chamber, thermal gradients in the gas existed axially. This field remained stationary, ensuring roughly the same parameter set for each probe tested.

#### 4. Results

Regarding thermodynamics, first the same testing method as introduced by us previously [16] was applied (while others used this approach as well [11,18–20]) and secondly – an approach similar to [12] was introduced. Concerning the first, the LBE was cooled from 550 to 300 °C (Fig. 1). The low cooling rate was as usual 2 K/min. This experiment has been repeated three times (runs 1–3). In Fig. 1 the dashed lines represent the theoretical EMF( $T$ ) dependencies for unsaturated solutions of oxygen in LBE, the concentrations given in wppm. The full line represents the saturation case. The probe responded accordingly to the oxygen content in the melt, but in the first run reaching the tangential point of saturation later than in the following runs, where more oxygen was dissolved allowing so the cooling curve to

reach the saturation line promptly. The registered plots for  $Bi/Bi_2O_3$  probes are in agreement with according nomograms – this for the whole range of over 200° (depending on the point of coincidence) down to  $\approx 300$  °C. Wu and Li reported 350 °C as their operating  $T_{min}$  [18].

In our kinetic studies first the LBE was deoxidised, subsequently moderate air ingress was performed and consequently the valve was closed leaving the system as such for  $\approx 3$  d without further gas flow until  $Ar/H_2$  bubbling was introduced and let as such for 8 h once again. The procedure was repeated several times, beginning with the flow of  $Ar/H_2$  provided for next 8 h. The changes in the  $Bi/Bi_2O_3$ -probe-EMFs exhibited *prompt responses* being reversible upon the gas changes in the KOSIMA-AT device. The same is observed as a result of basic studies in which phase equilibria between the oxygen dissolved in LBE and gaseous  $O_2$  were established for different  $H_2/H_2O$  atmospheres. Also, the sensor steady state responses are nearly the same for the stepwise increase/decrease in the  $H_2/H_2O$  ratio from 1.0 to 4.0 and vice versa. Comparing experimental EMFs with the predicted ones (Eq. (7)) shows a good agreement (Fig. 2). The differences between the steady state EMFs and the theoretical envelope were much lower than 10 mV in each case of an expected global variation of 50 mV. These EMFs approach nearly asymptotically the predicted levels of the calculated envelope for in-/decrease in the  $H_2/H_2O$  ratio. Moreover, the

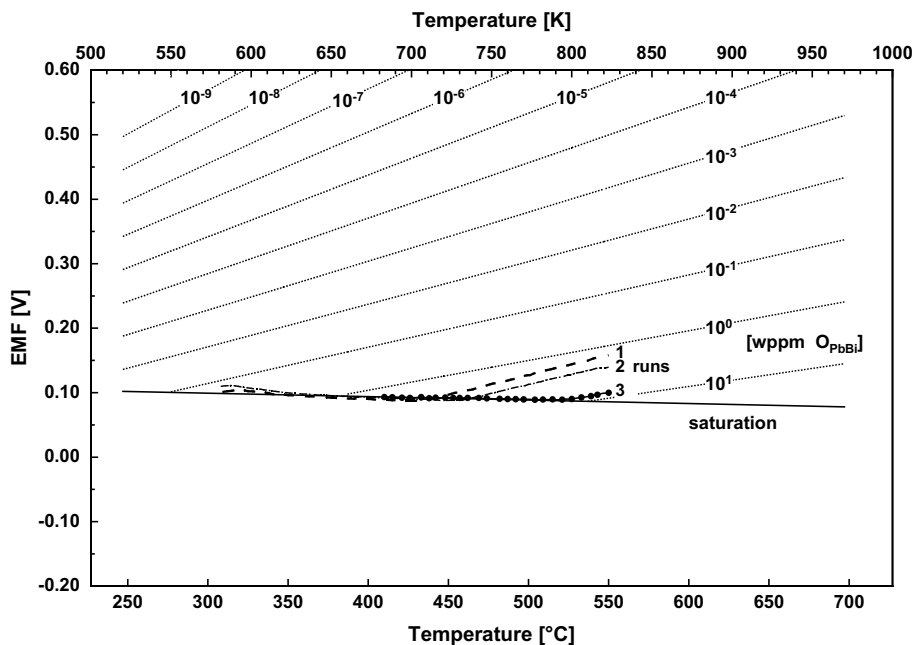


Fig. 1. Comparison of calculated and measured EMFs for an oxygen probe with  $Bi/Bi_2O_3$  reference electrode (subsequent cooling-down experiments).

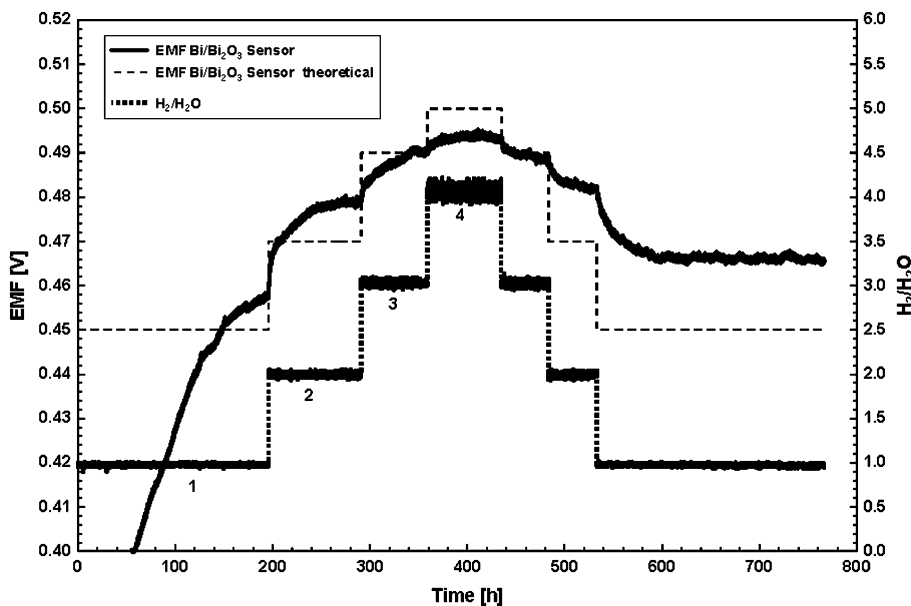


Fig. 2. The Bi/Bi<sub>2</sub>O<sub>3</sub> system – comparison between EMF( $\tau$ ) predicted (theoretical) and measured.

transient state – exponentially in nature – was convex and concave in shape for the former and latter, respectively. At a given H<sub>2</sub>/H<sub>2</sub>O ratio, the mean time constants for the uptake and the release of oxygen by the melt are almost the same indicative for the reversibility of processes occurring probably across the gas/LM surface- and surface/bulk-LM boundary layers. The overall time constants,  $k_f$  and  $k_b$  could be obtained assuming for simplicity first order kinetics. Having achieved an EMF limit the system was subject to the next change in the H<sub>2</sub>/H<sub>2</sub>O ratio – all the transients exhibited a similar appearance. The setting of  $p_{O_2}$  levels (gas) were deterministic even for changes in the H<sub>2</sub>/H<sub>2</sub>O ratio lower than one order of magnitude, nevertheless some noise was detected here by the ZIROX-device. The time needed for attaining equilibrium depended on the oxygen content in the LM. Comparing the results of the Bi/Bi<sub>2</sub>O<sub>3</sub> probe with that of the Pt/air probe [14] in the same melt, a similar kinetics is observed for 550 °C (Fig. 3). Shortly after starting the Ar/5%-H<sub>2</sub> bubbling, a sudden decrease of both the oxygen concentration  $c_O$  [wppm O] and/or the conjugated activity  $a_O$  in the LBE (evaluated via the EMFs) was detected by all probes. Air bubbling causes changes in the opposite direction. The EMF steady state of the oxygen saturation remains constant for the whole air bubbling period. The EMFs – output in mV – depend on the reference (Pt/air or Bi/Bi<sub>2</sub>O<sub>3</sub>), but – and that is significant and new – for quite different reference types the corresponding calculated values expressed as Nernstian  $p_{O_2}$  produced – for long time periods – nearly identical transients both in magnitude

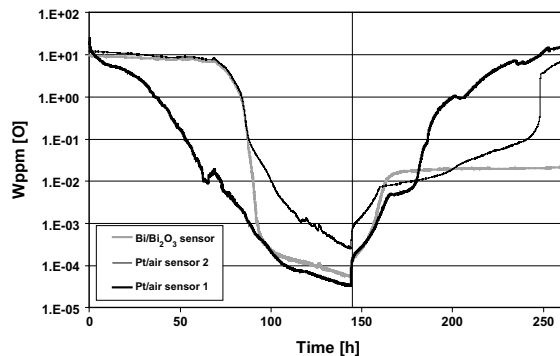


Fig. 3. Changes of EMF for a set of oxygen probes with two Pt/air and one Bi/Bi<sub>2</sub>O<sub>3</sub> system due to bubbling of oxidising (right) and reducing (left) gases through the LBE. Sensor outputs are normalized to oxygen concentration.

and slope (except for one Bi/Bi<sub>2</sub>O<sub>3</sub>-sensor giving for reasons unknown a different asymptotic line in case of oxidation). However, a delay in the response of one Pt/air probe compared to another identical Pt/air sensor is seen, likely caused by inhomogeneities in the melt along the lance with its orifices. Also, the oxygen uptake introduced via the lance is obviously enhanced at the site where the second probe is located despite the melt mixing using an agitator. In the context of that delay in sensing further preliminary tests at lower gas flow (10 cm<sup>3</sup>/min) were performed, showing a better performance.

## 5. Discussion and conclusions

Most significant is the fast response of the Bi/Bi<sub>2</sub>O<sub>3</sub> probe upon stepwise changing the H<sub>2</sub>/H<sub>2</sub>O ratios (Fig. 2) and lowering temperature (Fig. 1) in good agreement with the predicted Nernstian EMFs. The functioning of Bi/Bi<sub>2</sub>O<sub>3</sub>-probes down to 300 °C (closest to the melting point of Bi) is encouraging since such probes perform usually well at temperatures 50 °C higher [18]. On the other hand, reproducible non-linearities above 470 °C were caused exclusively by oxygen undersaturation. Tests have confirmed, that the calibration method postulated previously for Pt/air is suitable for Bi/Bi<sub>2</sub>O<sub>3</sub>-probes as well. Small stepwise changes of the H<sub>2</sub>/H<sub>2</sub>O ratio in opposite directions allow to determine some kinetics of oxygen transport from the gas towards the LM-bulk and vice versa. The EMF outputs were satisfactory. Testing several sensors in the same stagnant bath was done for online meter-to-meter comparison. Identical sensors have to give the same responses. However, to correlate the LM-*a*<sub>O</sub> data (stagnant case) with the adjusted gas-*p*<sub>O<sub>2</sub></sub> was more difficult as expected, since LM-inhomogeneities were observed. Which kind of transport phenomena necessitates correction factors and how they are to obtain is not clear yet. A dedicated mass-transfer modelling exclusively for KOSIMA-AT is considered to explain the observed oxygen spacial distribution in the LBE with respect of geometry, causing a defined bubble size distribution, bubble frequencies resulting from the total flow rate etc. In that context dynamic (loop) experiments are easier to perform, since better homogeneity of the solution is given. The probes tested responded rapidly to parameter changes. The EMF outputs are in agreement with the theoretically predicted ones, some shifts from the theoretical asymptotes could exceptionally be observed, however. The KOSIMA-AT facility designed for tests under stagnant conditions and equipped with several lab-designed and commercial Pt/air as well as Bi/Bi<sub>2</sub>O<sub>3</sub> sensors exhibited quite accurate and reversible *p*<sub>O<sub>2</sub></sub> and *a*<sub>O</sub> levels (EMFs within a narrow 10 mV tolerance limit). Sensors degradation was not observed during the tests, each of them up to ≈1000 h. The gas exchange system installed was fast enough to describe kinetic details. In agreement with Russian results [11] the use of Pt/air and Bi/Bi<sub>2</sub>O<sub>3</sub> in flowing LBE seems recommendable, nevertheless further loop experience must be acquired to enable proper judgement. Such tests are currently carried out in our CORRIDA loop.

## Acknowledgments

The work was performed in the EU TECLA Project framework and supported by the Nuclear Safety Program of the Forschungszentrum Karlsruhe.

## References

- [1] J. Konys (Ed.), Minutes of the Workshop on Heavy Liquid Metal Technology, 16–17 September 1999, Forschungszentrum Karlsruhe, Wissenschaftliche Berichte FZKA 6389.
- [2] K. Kiukolla, C. Wagner, *J. Electrochem. Soc.* 104 (1957) 308, 379.
- [3] A. Ramanarayanan, in: C. Subbarao (Ed.), *Limiting Factors in Measurements using the EMF Method in Solid Electrolytes and their Applications*, Plenum, NY, 1980, p. 81ff.
- [4] H.U. Borgstedt, C.K. Mathews, *Applied Chemistry of the Alkali Metals*, Plenum, NY, 1987.
- [5] B.A. Shmatko, N.I. Loginov, A.E. Rusanov, A.L. Shimkevich, *HLMC-98*, Obninsk 5–9 October 1998, p. 683.
- [6] V. Ghetta, F. Gamaoun, J. Fouletier, M. Hénault, A. Lemoulec, *J. Nucl. Mater.* 296 (2001) 295.
- [7] A. Chang, K. Fitzner, *Progr. Mater. Sci.* 32 (1988) 97, and the cited references therein.
- [8] V. Ghetta, J. Fouletier, M. Henault, A. Le Moulec, *J. Phys. IV France* 12 (2002) 123, Pr8.
- [9] H. Muscher, J. Konys, Z. Voß, O. Wedemeyer, *Wissenschaftliche Berichte FZKA 6690* (2001) and the cited references therein.
- [10] G. Müller, A. Heinzl, G. Schumacher, A. Weisenburger, *J. Nucl. Mater.* 321 (2003) 256.
- [11] B.A. Shmatko, A.E. Rusanov, *Mater. Sci.* 36 (5) (2000) 689.
- [12] N.A. Gokcen, J. Chipman, *J. Metals* 4 (1952) 171.
- [13] O. Kubaschewski, C.B. Alcock, *Metallurgical Thermochemistry*, Pergamon, London, 1958, p. 132.
- [14] R.C. Agarwala, A.K. Jena, *Z. Metallk.* 91 (5) (2000) 366.
- [15] J.A. Fernández, J. Abellà, J. Barceló, L. Victori, *J. Nucl. Mater.* 301 (2002) 47.
- [16] J. Konys, H. Muscher, Z. Voß, O. Wedemeyer, *J. Nucl. Mater.* 296 (2001) 289.
- [17] C.H. Lefhalm, J.U. Knebel, K.J. Mack, *J. Nucl. Mater.* 296 (2001) 301.
- [18] X. Wu R. Sivaraman, Ning Li, T.W. Darling, et al., in: *Int. Conf. Materials II, LBE Corrosion (East Madrone)*, 2–5.04.2003.
- [19] J.-L. Courouau, P. Trabuc, G. Laplanche, Ph. Deloffre, P. Taraud, M. Ollivier, R. Adriano, S. Trambaud, *J. Nucl. Mater.* 301 (2002) 53.
- [20] J.-L. Courouau, P. Deloffre, R. Adriano, *J. Phys. IV France* 12 (2002) 141, Pr8.